

# Controlling the Self-Assembly of a Mixed-Metal Mo/V–Selenite Family of Polyoxometalates

M. Nieves Corella-Ochoa, Haralampos N. Miras, De-Liang Long, and Leroy Cronin<sup>\*[a]</sup>

**Abstract:** Five mixed-metal mixed-valence Mo/V polyoxoanions, templated by the pyramidal  $\text{SeO}_3^{2-}$  heteroanion have been isolated:  $\text{K}_{10}[\text{Mo}_{12}^{\text{VI}}\text{V}_{10}^{\text{V}}\text{O}_{58}(\text{SeO}_3)_8]\cdot 18\text{H}_2\text{O}$  (**1**),  $\text{K}_7[\text{Mo}_{11}^{\text{VI}}\text{V}_5^{\text{V}}\text{V}_2^{\text{IV}}\text{O}_{52}(\text{SeO}_3)]\cdot 31\text{H}_2\text{O}$  (**2**),  $(\text{NH}_4)_7\text{K}_3[\text{Mo}_{11}^{\text{VI}}\text{V}_5^{\text{V}}\text{V}_2^{\text{IV}}\text{O}_{52}(\text{SeO}_3)](\text{Mo}_6^{\text{V}}\text{V}_6^{\text{V}}\text{O}_{22})\cdot 40\text{H}_2\text{O}$  (**3**),  $(\text{NH}_4)_{19}\text{K}_3[\text{Mo}_{20}^{\text{VI}}\text{V}_{12}^{\text{V}}\text{V}_4^{\text{IV}}\text{O}_{99}(\text{SeO}_3)_{10}]\cdot 36\text{H}_2\text{O}$  (**4**) and  $[\text{Na}_3(\text{H}_2\text{O})_5[\text{Mo}_{18-x}\text{V}_x\text{O}_{52}(\text{SeO}_3)]]\{\text{Mo}_{9-y}\text{V}_y\text{O}_{24}(\text{SeO}_3)_4\}$  (**5**). All five compounds were characterised by single-crystal X-ray structure analysis, TGA, UV/Vis and FT-IR spectroscopy, redox titrations, and elemental and flame atomic

absorption spectroscopy (FAAS) analysis. X-ray studies revealed two novel coordination modes for the selenite anion in compounds **1** and **4** showing  $\eta, \mu$  and  $\mu, \mu$  coordination motifs. Compounds **1** and **2** were characterised in solution by using high-resolution ESI-MS. The ESI-MS spectra of these compounds revealed characteristic patterns showing distribution envelopes corre-

sponding to 2– and 3– anionic charge states. Also, the isolation of these compounds shows that it may be possible to direct the self-assembly process of the mixed-metal systems by controlling the interplay between the cation “shrink-wrapping” effect, the non-conventional geometry of the selenite anion and fine adjustment of the experimental variables. Also a detailed IR spectroscopic analysis unveiled a simple way to identify the type of coordination mode of the selenite anions present in POM-based architectures.

**Keywords:** molybdenum • polyoxometalates • selenites • self-assembly • vanadium

## Introduction

Polyoxometalates (POMs) are anionic metal oxide clusters of Mo, W, V and Nb that have attracted the attention of many research groups during the last two decades, owing to their remarkable structural and electronic properties,<sup>[1,2]</sup> but also to their diverse properties ranging from photochromism,<sup>[3]</sup> electrochromism,<sup>[4]</sup> and magnetism<sup>[5]</sup> to applications in catalysis<sup>[6]</sup> and medicine.<sup>[7]</sup> Their formation mechanism is governed by self-assembly processes that involve the condensation of  $\{\text{MO}_x\}$  units ( $M = \text{W}, \text{Mo}, \text{V}, \text{Nb}$ ) directed by the fine adjustment of a long list of experimental variables, such as pH, ionic strength, counterion and metal-ion type, temperature, continuous flow conditions, and so forth.<sup>[8–13]</sup>

On the other hand, mixed-addenda hetero-POMs (HPOMs) exhibit a variety of structural motifs and properties that arise from the interplay between different oxidation states, geometries, labilities of the addenda units and the templating effect of the heteroatoms present in the structure.<sup>[14d–f]</sup> Detailed studies of these compounds reveals an astonishing variety of novel phases arising from the combina-

tion of molybdenum and vanadium precursors. Such structural diversity is associated with the versatility introduced to the system by the vanadium metal centres, owing to their variety of oxidation states (III, IV and V) and coordination geometries (tetrahedral, square pyramidal and octahedral). These aspects, combined with the relative robustness and stabilising effect of the molybdenum-based building units, consequently influence the final architecture of the isolated materials.<sup>[14e,f]</sup> Depending on the geometry and concentration ratios of the Mo/V addenda in the presence of a heteroatom, different structural motifs have been reported: The Anderson  $\{\text{XM}_6\text{O}_{24}\}$  structural motif with an octahedral heteroatom  $\{\text{XO}_6\}$  in the centre of a six-membered cyclic poly-anion,<sup>[15]</sup> the Keggin  $\{\text{XM}_{12}\text{O}_{40}\}$  motif with one  $\{\text{XO}_4\}$  tetrahedral heteroanion occupying the central cavity<sup>[16]</sup> and the Wells–Dawson  $\{\text{X}_2\text{M}_{18}\text{O}_{62}\}$  motif with two  $\{\text{XO}_4\}$  tetrahedral heteroanions inside the inorganic metal cage,<sup>[17]</sup> are examples of the different architectures commonly found in HPOMs.

HPOMs and mixed-metal HPOMs, which incorporate non-conventional (non-tetrahedral) heteroanions, are relatively rare; for example, the catalytically active tungstato-periodate compound  $[\text{H}_3\text{W}_{18}\text{O}_{56}(\text{IO}_6)]^{6-}$ , with one periodate anion embedded in a  $\{\text{W}_{18}\text{O}_{54}\}$  Dawson-type shell,<sup>[18]</sup> and the twofold reduced Dawson anion  $[\text{Mo}_{18}\text{O}_{54}(\text{SO}_3)_2]^{6-}$ , which incorporates two pyramidal sulfite ( $\text{SO}_3^{2-}$ ) heteroanions and exhibits intriguing S···S interactions and thermochromic properties.<sup>[19]</sup> HPOMs with non-conventional heteroanions are less common and are limited mainly to tungstate-based materials, which are less labile and their lacunary species

[a] M. N. Corella-Ochoa, Dr. H. N. Miras, Dr. D.-L. Long, Prof. L. Cronin  
WestCHEM, School of Chemistry  
The University of Glasgow  
University Avenue, Glasgow G12 8QQ, Scotland (UK)  
Fax: (+44) 141-330-4888  
E-mail: L.Cronin@chem.gla.ac.uk

Supporting information for this article is available on the WWW under <http://dx.doi.org/10.1002/chem.201200912>.

display increased stability.<sup>[20]</sup> Only a few examples of molybdate,<sup>[21]</sup> vanadate,<sup>[14,22]</sup> palladate<sup>[23]</sup> and mixed-metal molybdovanadate clusters<sup>[14d-g]</sup> have been reported recently in the literature.

In an attempt to expand the non-conventional HPOM family containing more labile metal oxide units, we investigated the interaction of pyramidal heteroanions from Group 16 ( $\text{SO}_3^{2-}$  and  $\text{TeO}_3^{2-}$ ) with molybdenum/vanadium mixed-addenda systems. Our recent investigations on the interaction of the pyramidal sulfite heteroanion ( $r_{\text{at}}=1.03 \text{ \AA}$ ) with a mixed-metal system, led to the isolation of two unprecedented novel Dawson-based archetypes:  $[\text{Mo}^{\text{VI}}_{11}\text{V}^{\text{V}}_5\text{V}^{\text{IV}}_2\text{O}_{52}(\mu_9\text{-SO}_3)]^{7-}$  ( $\{\text{M}_{18}\text{S}\}$ ) and  $[\text{Mo}^{\text{VI}}_{11}\text{V}^{\text{V}}_5\text{V}^{\text{IV}}_2\text{O}_{52}(\mu_9\text{-SO}_3)(\text{Mo}^{\text{V}}_6\text{V}^{\text{VO}}_{22})]^{10-}$  ( $\{\text{M}_{25}\text{S}\}$ ),<sup>[14d,e]</sup> whereas the incorporation of the tellurite anion ( $r_{\text{at}}=1.37 \text{ \AA}$ ) directed the self-assembly process towards the formation of two unique  $\text{M}_{24}$  cages,  $[\text{Mo}^{\text{VI}}_{12}\text{V}^{\text{V}}_8\text{V}^{\text{IV}}_4\text{Te}^{\text{IV}}\text{O}_{69}(\mu_9\text{-TeO}_3)_2]^{10-}$  ( $\{\text{M}_{24}\text{Te}_3\}$ ) and  $[\text{Mo}^{\text{VI}}_{12}\text{V}^{\text{V}}_8\text{V}^{\text{IV}}_4\text{O}_{69}(\mu_9\text{-TeO}_3)_2]^{14-}$  ( $\{\text{M}_{24}\text{Te}_2\}$ ) and one  $\{\text{M}_{25}\text{Te}\}$  archetype,  $[\text{Mo}^{\text{VI}}_{11}\text{V}^{\text{V}}_5\text{V}^{\text{IV}}_2\text{O}_{52}(\mu_9\text{-TeO}_3)(\text{Mo}^{\text{V}}_6\text{V}^{\text{VO}}_{22})]^{10-}$ .<sup>[14f]</sup> Based on our previously reported studies, we theorise that the influence of the pyramidal geometry, along with the ionic radius of the anion, can have a powerful effect on the self-assembly processes and consequently allow the design of new structural motifs. Additionally, the stereochemically active lone pair of electrons on the heteroanion can potentially facilitate or induce interesting redox and photophysical properties onto the cluster oxide shell.<sup>[18,24]</sup> This means that the extension of the family of these compounds, that is, to explore the influence of the selenite anion ( $\text{SeO}_3^{2-}$ ), on the self-assembly of mixed addenda POM systems should allow a correlation between the pyramidal geometry, the ionic radius and the observed structural motifs.

Herein, we report the isolation of five new selenite-based polyoxometalates:  $\{\text{M}_{22}\text{Se}_8\} = \text{K}_{10}[\text{Mo}^{\text{VI}}_{12}\text{V}^{\text{V}}_{10}\text{O}_{58}(\text{SeO}_3)_8] \cdot 18\text{H}_2\text{O}$  (**1**),  $\{\text{M}_{18}\text{Se}\} = \text{K}_7[\text{Mo}^{\text{VI}}_{11}\text{V}^{\text{V}}_5\text{V}^{\text{IV}}_2\text{O}_{52}(\mu_9\text{-SeO}_3)] \cdot 31\text{H}_2\text{O}$  (**2**) and  $\{\text{M}_{25}\text{Se}\} = (\text{NH}_4)_7\text{K}_3[\text{Mo}^{\text{VI}}_{11}\text{V}^{\text{V}}_5\text{V}^{\text{IV}}_2\text{O}_{52}(\mu_9\text{-SeO}_3)(\text{Mo}^{\text{V}}_6\text{V}^{\text{VO}}_{22})] \cdot 40\text{H}_2\text{O}$  (**3**);  $\{\text{M}_{36}\text{Se}_{10}\} = (\text{NH}_4)_{19}\text{K}_3[\text{Mo}^{\text{VI}}_{20}\text{V}^{\text{V}}_{12}\text{V}^{\text{IV}}_4\text{O}_{99}(\text{SeO}_3)_{10}] \cdot 36\text{H}_2\text{O}$  (**4**), which, to the best of our knowledge, is the first mixed-metal Mo/V lacunary-type cluster templated by a pyramidal heteroanion as well as the largest Mo/V-selenite-based POM reported to date; and  $[\text{Na}_3(\text{H}_2\text{O})_5\{\text{Mo}_{18-x}\text{V}_x\text{O}_{52}(\mu_9\text{-SeO}_3)\}\{\text{Mo}_{9-y}\text{V}_y\text{O}_{24}(\text{SeO}_3)_4\}]$  (**5**). All compounds were synthesised under one-pot reaction conditions, for which the pH and the cation effect proved to be the determining factors for the reproducible control of the self-assembly process (Figure 1). The compounds were characterised by X-ray structural analysis, TGA, UV/Vis and FT-IR spectroscopy, FAAS, redox titrations and ESI-MS. A detailed spectroscopic analysis of the FT-IR spectra for all five compounds, identifying the different coordination modes of the selenite heteroanions exhibited in the observed architectures is also reported.

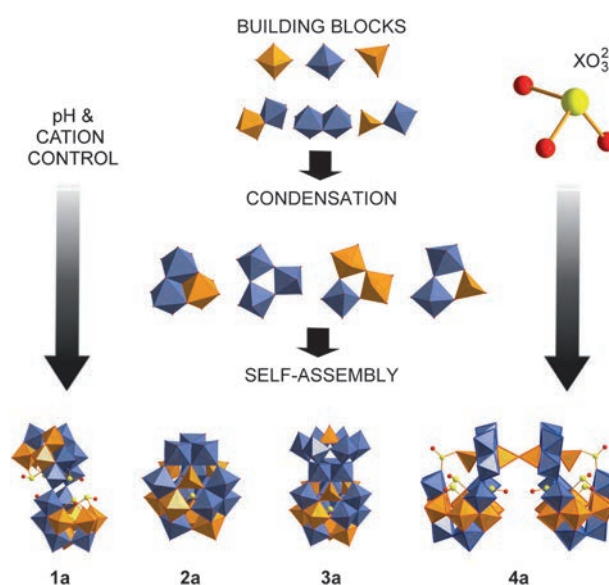
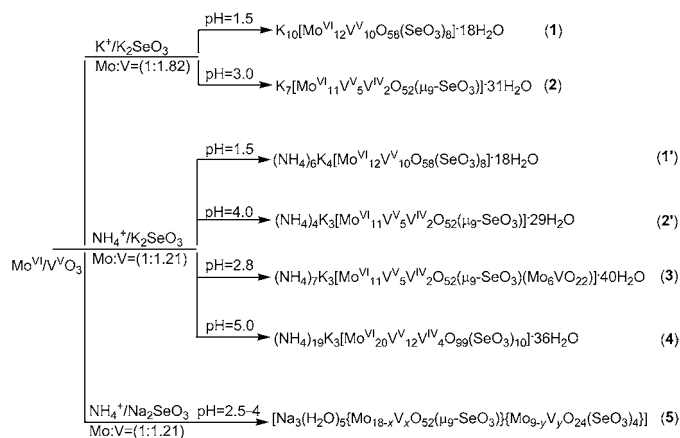


Figure 1. Representation of the self-condensation of the different building units involved in the reaction mixtures leading to the isolation of a new family of HPOM clusters templated by the pyramidal selenite heteroanion  $\text{SeO}_3^{2-}$ . Mo: purple, V: orange, Se: yellow sphere and O: red sphere.

## Results and Discussion

**Syntheses:** The procedures followed for the synthesis of compounds **1**, **1'**, **2**, **2'**, **3** and **4** are summarised in Scheme 1. Compound **1** was prepared by the sequential addition of  $\text{KVVO}_3$ ,  $\text{K}_2\text{SeO}_3$  and  $\text{NH}_2\text{NH}_2 \cdot 2\text{HCl}$  to a hot aqueous solution containing  $\text{K}_2\text{Mo}^{\text{VI}}\text{O}_4$ . The reaction was allowed to cool to room temperature and the pH was then adjusted to 1.5 by the drop-wise addition of a 3M HCl solution. Dark orange rhomboid crystals of  $\text{K}_{10}[\text{Mo}^{\text{VI}}_{12}\text{V}^{\text{V}}_{10}\text{O}_{58}(\text{SeO}_3)_8] \cdot 18\text{H}_2\text{O}$  (**1**) formed after two days. Crystals of **1** were removed from the solution and the mother liquor was left to evaporate at room temperature for three days during which period of time dark hexagonal crystals of  $\text{K}_7[\text{Mo}^{\text{VI}}_{11}\text{V}^{\text{V}}_5\text{V}^{\text{IV}}_2\text{O}_{52}(\mu_9\text{-SeO}_3)] \cdot 31\text{H}_2\text{O}$  (**2**) were isolated. Al-



Scheme 1. Synthetic procedure for the formation of compounds **1–5**.

ternatively, mapping the reaction conditions of the  $K^+/Mo/V$  system over a wide range of pH values, led to the direct synthesis of compound **2** at a pH value of 3 in the presence of  $NH_2NH_2 \cdot 2HCl$  as reducing agent.

From our previously reported studies, we demonstrated the impact of the cation effect on the self-assembly process of the available building units.<sup>[14e,f,25b]</sup> Based on this fact, we decided to investigate the self-assembly processes in the presence of other cations that could influence the type of available building block libraries as well as their aggregation by means of a network of hydrogen-bonding interactions, electrostatic and “shrink-wrapping” effects.<sup>[25]</sup> The successive addition of  $NH_4VO_3$ ,  $K_2SeO_3$  and  $NH_2NH_2 \cdot 2HCl$  into an acidic solution of  $(NH_4)_6Mo^{VI}_7O_{24}$  led to the formation of four new compounds after adjusting the pH of the mixture by addition of 3 M HCl. The co-operative effect of the reducing agent and the pH value is a known crucial parameter in POM chemistry.<sup>[1,2]</sup> Reduction of the vanadium centres is important for the initiation of the self-assembly process, since it is more reactive and triggers the formation of a building block library. On the other hand, the pH value controls and drives finally the condensation process of the available building units towards the formation of the final product. Fine adjustment of the pH value of the solution to 1.5, yielded crystals of  $(NH_4)_6K_4[Mo^{VI}_{12}V^{V}_{10}O_{58}(SeO_3)_8] \cdot 18H_2O$  (**1'**) within a week. When the pH was increased to 2.8, crystals of  $(NH_4)_4K_3[Mo^{VI}_{11}V^{V}_5V^{IV}_2O_{52}(\mu_9-SeO_3)] \cdot 29H_2O$  (**2'**) along with crystals of  $(NH_4)_7K_3[Mo^{VI}_{11}V^{V}_5V^{IV}_2O_{52}(\mu_9-SeO_3)(Mo^V_6V^VO_{22})] \cdot 29H_2O$  (**3**) were collected, after standing for a period of two weeks.

In an effort to avoid co-crystallisation of compounds **2'** (large hexagonal crystals) and **3** (needle crystals) we investigated the system over a wide range of pH values, and we managed to isolate a pure phase of compound **2'** by adjusting the pH value between 4 and 4.5, whereas between 2.8 and 4.0 the species continue to co-crystallise.

Since we were not able to determine appropriate synthetic conditions for the isolation of the pure crystalline phase of compound **3**, we separated the needle-shaped crystals of **3** manually under the microscope. The separation is relatively facile due to their considerably different size and shape (compound **2'** gives large hexagonal crystals).

When the pH was increased to a value of 5.0, crystals of the largest mixed-addenda lacunary selenite species  $(NH_4)_{19}K_3[Mo^{VI}_{20}V^{V}_{12}V^{IV}_4O_{99}(SeO_3)_{10}] \cdot 36H_2O$  (**4**) were formed after ten days; whereas if the pH value was increased further to 6.0, yellow crystals of  $K_7[Mo^{VI}_8V^{V}_5O_{40}] \cdot 9H_2O$  were formed instead.<sup>[26]</sup> Above the pH value of 6.0, a rapid oxidation of the reaction mixture was observed and only crystals of decavanadate ( $[V_{10}O_{28}]^{6-}$ ) were obtained, with different extents of protonation, depending on the basicity of the solution.<sup>[27]</sup>

In an effort to expand our investigation of the cation effect on the self-assembly process, we replaced the potassium source ( $K_2SeO_3$ ) by a sodium source ( $Na_2SeO_3$ ) and observed that small amounts of crystals of  $[Na_{3-x}(H_2O)_5\{Mo_{18-x}V_xO_{52}(\mu_9-SeO_3)\}\{Mo_{9-y}V_yO_{24}(SeO_3)_4\}]$  (**5**)

were formed in the pH range of 2.5 and 4 after two weeks. Under these experimental conditions, in the presence of a  $Na^+/NH_4^+$  cation mixture, compound **5** always co-crystallised with the decavanadate  $[V_{10}O_{28}]^{6-}$  species, along with  $[Mo^{VI}_{12}V^{V}_{10}O_{58}(SeO_3)_8]^{10-}$  and  $[Mo^{VI}_{11}V^{V}_5V^{IV}_2O_{52}(\mu_9-SeO_3)]^{7-}$  crystals, which are isostructural to **1** and **2**, respectively. At this point it is worth noting the following observations: 1) the fine tuning of the experimental parameters and the careful reaction mapping of the mixed addenda system was crucial for the discovery of the novel family of selenite-based POMs; 2) the interplay between the geometrical factors [ionic radius ( $r_{at}$ ) = 1.17 Å] and the pyramidal geometry] of the selenites and the “shrink-wrapping” effect of the cation influenced the self-assembly process, leading to the formation of high-nuclearity mixed-metal oxides such as  $\{M_{22}Se_8\}$  and  $\{M_{36}Se_{10}\}$ ; and 3) we have been able to unveil a series of novel coordination modes of the selenite anion, demonstrating its ability to act effectively as inorganic ligand. This has a profound effect on the self-assembly process of the available synthons involved in the reaction mixture, leading to the discovery of a range of unprecedented structural motifs.

#### Structural description of the selenite–molybdovanadate clusters:

The crystallographic parameters for the compounds **1–5** are listed in Tables 4 and 5 in the Experimental Section. Crystallographic studies revealed that the anion in **1** can be formulated as  $[Mo^{VI}_{12}V^{V}_{10}O_{58}(SeO_3)_8]^{10-}$  (**1a**), which adopts an S-shaped topology similar to the 22-isopolytungstate cluster  $[H_4W_{22}O_{74}]^{12-}$ ,<sup>[28]</sup> even though in the present case, the lacunary synthons are templated and bridged together by eight pyramidal selenite anions. The  $\{M_{22}Se_8\}$  cluster is built up from two  $\{M_{11}Se_4\}$  subunits linked by two  $\mu$ -oxo bridges in a *trans* fashion. Each bowl-shaped  $\{M_{11}Se_4\}$  subunit consists of a  $[Mo^{VI}_4V^V_5O_{24}(\mu_9-SeO_3)]^-$  cap, in which the top is decorated by a belt-shaped  $[Mo^{VI}_2Se^{IV}_3O_{14}]^{4-}$  moiety with alternating  $SeO_3^{2-}$  pyramids and  $MoO_6$  octahedra (Figure 2). Whilst the Mo atoms in the  $[Mo^{VI}_2Se^{IV}_3O_{14}]^{4-}$  fragment are crystallographically distinguishable, the metal sites in the  $\{M_9\}$  fragment are disordered over the nine positions. The assignment of formal charges on the metal ions was made on the basis of charge balance considerations for the entire compound, combined with bond valence sum (BVS) calculations,<sup>[14,29]</sup> redox titrations, elemental analysis, and high-resolution electrospray mass spectroscopy (ESI-MS). The Mo atoms in the  $[Mo^{VI}_2Se^{IV}_3O_{14}]^{4-}$  formation are in the oxidation state VI (BVS<sub>av</sub> = 5.82) and their coordination sphere is completed by two terminal oxo groups in *cis* positions, with an average Mo=O bond length of 1.70(1) Å, one  $\mu$ -O<sup>2-</sup> groups, with Mo–O bond lengths of 1.90(8) Å, and three  $\mu_3$ -O<sup>2-</sup> bridges, with Mo–O bonds spanning 1.98(1)–2.28(1) Å. A feature of the  $\{M_{22}Se_8\}$  cluster worth noting is the incorporation of eight  $SeO_3^{2-}$  heteroanions with three distinct coordination modes (Figure 3): a) one  $\mu_9$ - $SeO_3$  anion occupies the central cavity of each  $\{M_9\}$  unit; b) and c) one ( $\mu, \mu$ )- $SeO_3$  and two ( $\eta, \mu$ )- $SeO_3$  bridging anions are incorporated in the  $[Mo^{VI}_2Se^{IV}_3O_{14}]^{4-}$  formation, respectively. These are

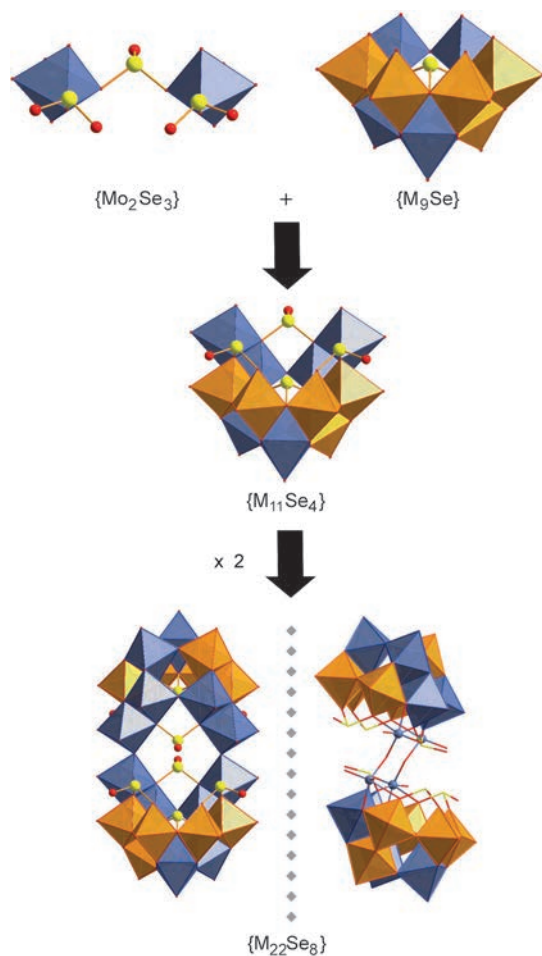


Figure 2. Polyhedral representation of **1a** built up from two  $\{M_{11}Se_4\}$  units connected together by two  $\mu_2$ -oxo bridges in a *trans* fashion (purple spheres). Mo: purple, V: orange, Se: yellow sphere and O: red sphere.

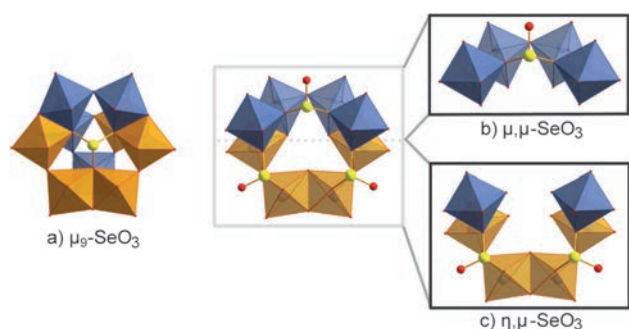


Figure 3. Coordination modes from the  $SeO_3^{2-}$  anion found in **1a**. Mo: purple, V: orange, Se: yellow sphere and O: red sphere.

two novel modes for the selenite anion and are reported for the first time. All the Se atoms exhibit the formal oxidation state IV ( $BVS_{av} = 3.94$ ). Bond lengths relevant to the coordination sphere of the Se atoms in the  $SeO_3$  pyramidal polyhedra are given in Table 1.

Table 1. Selected interatomic distances and angles relevant to the coordination sphere for selenite atoms in compound **1** (see in the Supporting Information for atom labelling).

bond lengths [Å]			
Se(1)–O(16)	1.69(1)	Se(2)–O(21)	1.77(1)
Se(1)–O(16 A)	1.69(1)	Se(3)–O(30)	1.70(1)
Se(1)–O(17)	1.69(1)	Se(3)–O(9)	1.76(1)
Se(2)–O(5)	1.62(1)	Se(3)–O(9 A)	1.76(1)
Se(2)–O(20)	1.72(1)		
angles [°]			
O(16)–Se(1)–O(16 A)	98.1(9)	O(20)–Se(2)–O(21)	98.6(6)
O(16)–Se(1)–O(17)	99.3(6)	O(30)–Se(3)–O(9)	117.2(1)
O(16 A)–Se(1)–O(17)	99.3(6)	O(30)–Se(3)–O(9 A)	117.2(1)
O(5)–Se(2)–O(20)	106.3(7)	O(9)–Se(3)–O(9 A)	102.8(9)
O(5)–Se(2)–O(21)	103.0(7)		

As we discussed earlier, the  $\{M_{22}Se_8\}$  anion could be synthesised over a wide range of pH values utilising different cations that appeared to promote the self-assembly process. Based on the electrostatic interactions and network of hydrogen bonds formed between the building units and the cations, it was possible to crystallise anion **1a** in different space groups, and consequently different packing motifs. When potassium was used as a cation, compound **1** crystallised in the space group  $C2/m$  in which every  $\{M_{22}Se_8\}$  unit is connected to each other by means of potassium cations forming a 2D sheet (Figure 4a). When ammonium and potassium cations were present, compound **1'** crystallised in the  $C2/c$  space group and every  $\{M_{22}Se_8\}$  cluster is connected through potassium cations to the neighbouring one in a zigzag fashion, forming infinite 1D chains (Figure 4b).

The anion of compound **2** can be formulated as  $[Mo^{VI}_{11}V^V_5V^{IV}_2O_{52}(\mu_9-SeO_3)]^{7-}$  (**2a**) and is isostructural to the sulfite-based Dawson-like structure  $[Mo^{VI}_{11}V^V_5V^{IV}_2O_{52}(\mu_9-SO_3)]^{7-}$  (Figure 6a, see later).<sup>[14e]</sup> The disordered egg-

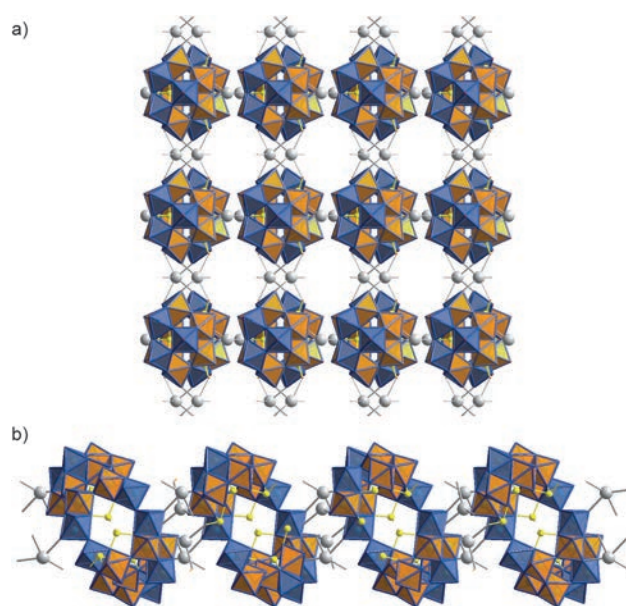


Figure 4. Packing modes for **1a**: a)  $C2/m$  (view from the *a* axis), b)  $C2/c$  (view along *b* axis). Mo: purple, V: orange, Se: yellow and K: grey.

shaped cage can be split in two hemispheres. The upper hemisphere consists of three edge-sharing  $\text{MoO}_6$  octahedra connected to the upper belt through vertexes of alternating  $\text{V}^{\text{V}}\text{O}_4$  tetrahedra and  $\text{MoO}_6$  octahedra. The remaining four V positions (two  $\text{V}^{\text{V}}$  and two  $\text{V}^{\text{IV}}$ ) are crystallographically disordered over the nine  $\text{MO}_6$  octahedral positions in the lower hemisphere of the cluster, and the cavity is occupied by a  $\mu_9\text{-SeO}_3^{2-}$  ion.

Whilst the Mo and V atoms are crystallographically distinguishable in the upper hemisphere, the metal sites in the lower hemisphere are crystallographically disordered. Therefore, the identification of the oxidation state of the metal centres was made on the basis of charge balance considerations for the entire compound, combined with bond valence sum (BVS) calculations,<sup>[14,29]</sup> redox titrations, elemental analysis, and high-resolution electrospray mass spectroscopy (ESI-MS). All the Mo atoms have the formal oxidation state VI ( $\text{BVS}_{\text{av}}=5.89$ ), the V atoms in the  $\text{VO}_4$  tetrahedra are in the oxidation state V ( $\text{BVS}_{\text{av}}=5.14$ ) and the Se atom in the  $\mu_9\text{-SeO}_3^{2-}$  is in the oxidation state IV ( $\text{BVS}=4.01$ ). The V atoms in the  $\text{VO}_4$  tetrahedra are coordinated by three  $\mu_3\text{-O}^{2-}$  moieties, with V–O bonds spanning the range 1.722(4)–1.755(4) Å, and one terminal oxo group, with a V=O bond length of 1.626(5) Å. The Mo atoms in the upper hemisphere exhibit two terminal oxo groups in *cis* positions, with Mo=O bond lengths in the range of 1.693(4)–1.718(4) Å, and one  $\mu\text{-O}^{2-}$  and three  $\mu_3\text{-O}^{2-}$  bridges, with Mo–O bonds between 1.873(4)–1.888(4) Å and 2.000(4)–2.264(4) Å, respectively. Utilisation of different cations, directed the crystallisation of anion **2a** in different space groups and consequently in different packing modes. When only potassium is used as a cation, the  $\{\text{M}_{18}\text{Se}\}$  cage crystallised in the  $P4b2$  space group (Figure 5 a), whereas if ammonium is also present in solution it crystallised in  $R\bar{3}c$  (Figure 5). The clusters in  $P4b2$  space group pack in a herringbone pattern of alternating rectangular ( $20.1 \times 4.4$  Å) and circular (3.2 Å) cavities, while the clusters in  $R\bar{3}c$  space group are organised in triads forming a equilateral triangular cavity between the  $\{\text{Mo}_{11}\text{V}_7\text{Se}\}$  clusters with dimensions of about 5.0 Å.

Compound **3** adopts the “crowned” Dawson-like structure, isostructural to the sulfite- and tellurite-based HPOMs reported recently,<sup>[14e,f]</sup> and the anion can be formulated as  $[\text{Mo}_{11}^{\text{VI}}\text{V}_5^{\text{V}}\text{V}_2^{\text{IV}}\text{O}_{52}(\mu_9\text{-SeO}_3)(\text{Mo}_6^{\text{V}}\text{V}^{\text{V}}\text{O}_{22})]^{10-}$  (**3a**). It is built up from two parts: a disordered egg-shaped capsule  $\{\text{Mo}_{11}^{\text{VI}}\text{V}_5^{\text{V}}\text{V}_2^{\text{IV}}\text{O}_{52}(\mu_9\text{-SeO}_3)\}$  identical to anion **2a** and a  $\{\text{Mo}_6^{\text{V}}\text{V}^{\text{V}}\text{O}_{22}\}$  crown attached to the top of the Dawson-like capsule through six oxo bridges (Figure 6 b).

The crown is formed from three pairs of corner-shared  $\text{MoO}_6$  octahedral units composed of two terminal oxo groups and one  $\text{VO}_4$  tetrahedral occupying the centre of the crown. Whilst the Mo and V atoms are crystallographically distinguishable in the crown and in the upper hemisphere of the Dawson-like capsule, the metal sites in the lower hemisphere are disordered over nine positions. Therefore, the assignment of formal charges on the metal ions was made on the basis of charge balance considerations for the entire

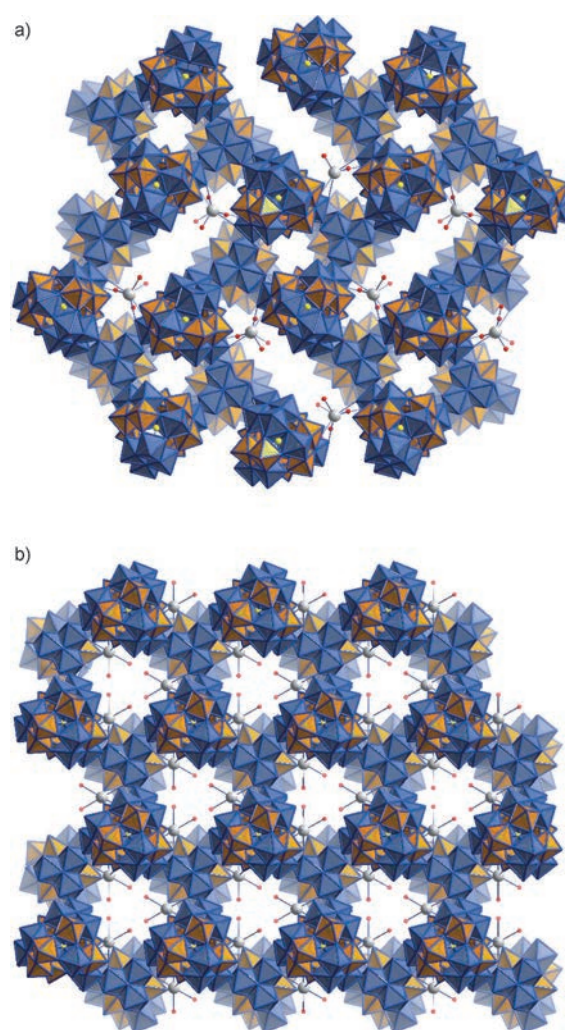


Figure 5. Packing modes for **2a**: a) in  $P4b2$  (view along *c* axis) and b) in  $R\bar{3}c$  (view along *c* axis). Mo: purple polyhedra, V: orange polyhedra, Se: yellow spheres and O: red spheres.

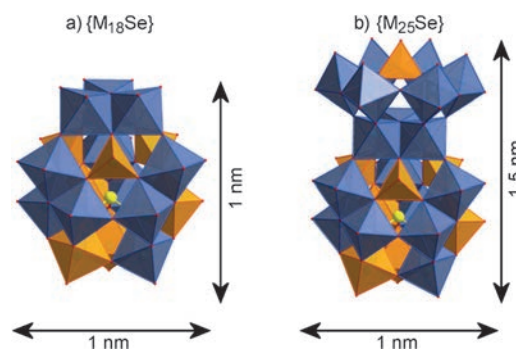


Figure 6. Polyhedral representation of a) anion **2a** and b) anion **3a**. Mo: purple, V: orange, Se: yellow sphere and O: red sphere.

compound, combined with bond valence sum (BVS) calculations,<sup>[14,29]</sup> redox titrations, elemental analysis, and high-resolution electrospray mass spectroscopy. All the Mo atoms have the formal oxidation state VI ( $\text{BVS}_{\text{av}}=6.12$ ), the V atoms in the  $\text{VO}_4$  tetrahedra are in the oxidation state V

( $BVS_{av}=5.14$ ) and the Se atom in the  $\mu_9$ - $SO_3$  in the oxidation state IV ( $BVS=3.94$ ). The V atoms in the  $VO_4$  tetrahedra are coordinated by three  $\mu_3$ - $O^{2-}$  moieties, with V–O bonds spanning the range 1.71(1)–1.78(1) Å and one terminal oxo group with the V=O bond length falling in the range of 1.61(1)–1.62(1) Å. Whilst the Mo atoms in the upper hemisphere exhibit two terminal oxo groups in *cis* positions, with Mo=O bond lengths in the range of 1.67(1)–1.69(1) Å, and one  $\mu$ - $O^{2-}$  and three  $\mu_3$ - $O^{2-}$  groups, with Mo–O bond lengths between 1.870(9)–1.880(1) Å and 1.990(1)–2.286(9) Å, respectively; the relevant Mo–O bonds in the crown formation appear to be slightly elongated with the two terminal oxo groups in *cis* positions spanning the range 1.68(1)–1.73(1) Å, and the three  $\mu$ - $O^{2-}$  and one  $\mu_3$ - $O^{2-}$  moieties, with Mo–O bond lengths between 1.890(1)–2.453(9) Å and 2.21(1)–2.23(1) Å, respectively.

X-ray crystallographic analysis of compound **4** revealed a novel lacunary molybdovanadate cluster with the general formula  $(NH_4)_{19}K_3[Mo^{VI}_{20}V^{V}_{12}V^{IV}_4O_{99}(SeO_3)_{10}]\cdot 36H_2O$  (**4**), which incorporates ten pyramidal heteroanions. It is a dimer of two “ $\delta$ ”-shaped  $[Mo_{10}^{VI}V^V_6V^{IV}_2O_{50}(SeO_3)_5]^{11-} = \{Mo_{10}V_8Se_5\}$  units (Figure 7a). Each  $\{Mo_{10}V_8Se_5\}$  unit can be

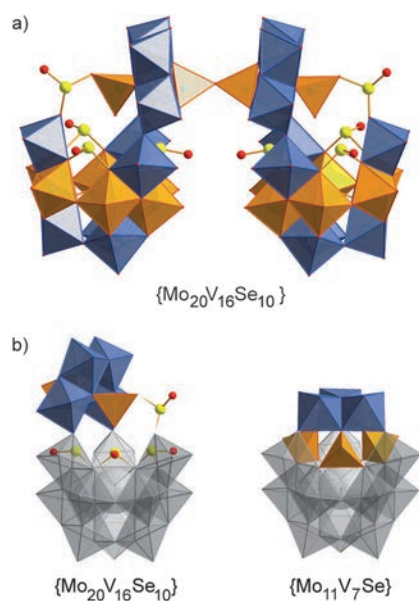


Figure 7. a) Polyhedral representation of anion **4a**, b) structural comparison with compound **2a**, in which the colourful polyhedral represent the substituted moieties. Mo: purple, V: orange, Se: yellow sphere and O: red sphere.

split in two hemispheres in a similar fashion as in the case of the egg-shaped Dawson archetype anion **2a**. The lower hemisphere is isostructural to **2a**, in which the Mo and V metal centres are crystallographically disordered over the nine  $\{MO_6\}$  octahedral positions. In the upper hemisphere the three  $VO_4$  tetrahedra from **2a** have been replaced in this case by three  $(\mu,\mu)$ - $SeO_3$  pyramidal anions, while the three edge-shared  $MoO_6$  octahedra of the cap have been replaced by two edge-shared molybdenum dimeric units and a

$\{VO_4\}$  pyramid tilted by approximately  $75^\circ$  owing to the incorporation of one  $VO_4$  tetrahedral unit and one  $SeO_3^{2-}$  pyramid forming the  $\{Mo_4V_2Se\}$  unit (Figure 7b), which decorates the top of the architecture.

The  $\{Mo_4V_2Se\}$  units are connected by three  $\mu$ - $O^{2-}$  bridges, one from the  $(\mu,\mu)$ - $SeO_3$  and two from the  $MoO_6$  units. The Mo and V atoms in the  $\{Mo_4V_2Se\}$  unit are crystallographically resolved. As in the previous cases, the identification of the oxidation state of the metal ions was made based on the overall charge of the compound, combined with bond valence sum (BVS) calculations,<sup>[14,29]</sup> redox titrations, and elemental analysis. All the Mo atoms have the formal oxidation state VI ( $BVS_{av}=5.92$ ), the V atoms in the  $VO_4$  tetrahedra are in the oxidation state V ( $BVS_{av}=5.15$ ) and the Se atoms are in the oxidation state IV ( $BVS_{av}=3.92$ ). The coordination sphere of the Mo atoms in the  $\{Mo_4V_2Se\}$  unit is completed by two terminal oxo groups in *cis* positions, with Mo=O bond lengths between 1.696(8)–1.717(9) Å; and the V atoms in the  $VO_4$  tetrahedra exhibit one terminal oxo group with an average V=O bond length falling in the range 1.590(8)–1.788(9) Å.

As in the case of anion **1a** it is worth noting the variety of coordination modes that the selenite heteroanion adopts within the same architecture (Figure 8). More specifically

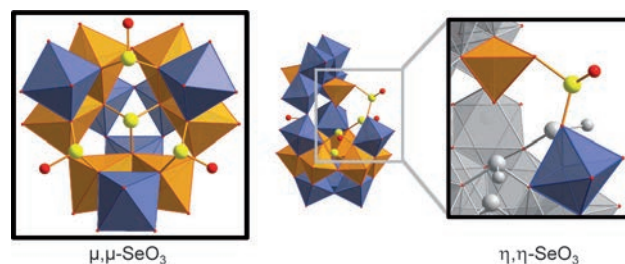


Figure 8. Coordination modes from the  $SeO_3^{2-}$  bridging anion found in **4a**. Mo: purple, V: orange, Se: yellow sphere and O: red sphere.

there is a) one  $\mu_9$ - $SeO_3^{2-}$  bridging anion that occupies the cavity and templates the formation of the lower hemisphere; b) three  $(\mu,\mu)$ - $SeO_3^{2-}$  bridging anions incorporated in the upper belt; and c) one  $(\eta,\eta)$ - $SeO_3$  bridging anion that bridges the cap  $\{Mo_4V_2Se\}$  with the lower hemisphere, while at the same time keeps the cap tilted by  $75^\circ$ ; d) the novel coordination mode— $(\mu,\mu)$ —is observed here as well. Bond lengths relevant to the coordination sphere of the Se atoms in the  $SeO_3$  pyramidal polyhedra are given in Table 2.

X-ray investigation of **5** revealed the following compound with the general formula  $[Na_3(H_2O)_5\{Mo_{18-x}V_xO_{52}(\mu_9-SeO_3)\}\{Mo_{9-y}V_yO_{24}(SeO_3)_4\}]$  (**5**). Due to the co-crystallisation of compound **5** with the anions **1a** and **2a** and also the different forms of the decavanadate anion, it was not possible to characterise compound **5** sufficiently and determine accurately the molecular formula of the title compound. However, based on the crystallographic data combined with bond valence sum calculations,<sup>[14,29]</sup> we can describe the anion **5a** as one  $\{Mo_{18-x}V_xO_{52}(\mu_9-SeO_3)\}$  unit, isostructural

Table 2. Selected interatomic distances and angles relevant to the coordination sphere for selenite atoms in compound **4** (see the Supporting Information for atom labelling).

bond lengths [Å]			
Se(1)–O(18)	1.700(7)	Se(3)–O(16)	1.748(7)
Se(1)–O(4)	1.702(7)	Se(4)–O(38)	1.648(7)
Se(1)–O(9)	1.707(7)	Se(4)–O(25)	1.726(7)
Se(2)–O(13)	1.646(8)	Se(4)–O(17)	1.738(7)
Se(2)–O(10)	1.727(7)	Se(5)–O(51)	1.57(1)
Se(2)–O(39)	1.730(7)	Se(5)–O(68)	1.67(1)
Se(3)–O(15)	1.642(7)	Se(5)–O(78)	1.843(9)
Se(3)–O(14)	1.746(7)		
angles [°]			
O(18)–Se(1)–O(4)	99.8(3)	O(14)–Se(3)–O(16)	98.0(3)
O(18)–Se(1)–O(9)	100.1(3)	O(38)–Se(4)–O(25)	103.6(4)
O(4)–Se(1)–O(9)	99.7(3)	O(38)–Se(4)–O(17)	103.4(4)
O(13)–Se(2)–O(10)	104.1(4)	O(25)–Se(4)–O(17)	99.0(4)
O(13)–Se(2)–O(39)	103.5(4)	O(51)–Se(5)–O(68)	120.0(10)
O(10)–Se(2)–O(39)	100.1(3)	O(51)–Se(5)–O(78)	107.6(7)
O(15)–Se(3)–O(14)	103.2(3)	O(68)–Se(5)–O(78)	111.8(5)
O(15)–Se(3)–O(1)	102.6(4)		

to **2a**, connected by three sodium cations to a  $\{\text{Mo}_{9-y}\text{V}_y\text{O}_{24}(\text{SeO}_3)_4\}$  unit, isostructural to the lacunary form of the Keggin  $[\text{XM}_9\text{O}_{34}]^{n-}$  archetype,<sup>[30]</sup> in which its lacunary positions are occupied in the present case by three  $(\eta,\eta)\text{-SeO}_3^{2-}$  bridging anions (Figure 9). Whereas all the Mo and V atoms are crystallographically disordered over the positions of the trivacant Keggin fragment and the lower hemisphere of the Dawson-like cluster, the upper hemisphere of the latter is well resolved with six Mo atoms in the  $\text{MoO}_6$  octahedra with formal oxidation state VI ( $\text{BVS}_{\text{av}}=5.95$ ) and three V atoms in the  $\text{VO}_4$  tetrahedra with oxidation state V ( $\text{BVS}_{\text{av}}=5.09$ ). All the Se atoms are in the oxidation state IV ( $\text{BVS}_{\text{av}}=3.97$ ). Additionally, the Mo dioxo positions exhibit average  $\text{Mo}=\text{O}$  bond lengths of 1.687(7)–1.711(7) Å, one  $\mu\text{-O}^{2-}$  moiety with  $\text{Mo}-\text{O}$  bond lengths falling in the range 1.875(7)–1.902(8) Å and three  $\mu_3\text{-O}^{2-}$  moieties with  $\text{Mo}-\text{O}$  bond lengths between 1.994(7)–2.278(7) Å and are in good agreement with the previously discussed compounds. The coordination environment of the V atoms in the  $\text{VO}_4$

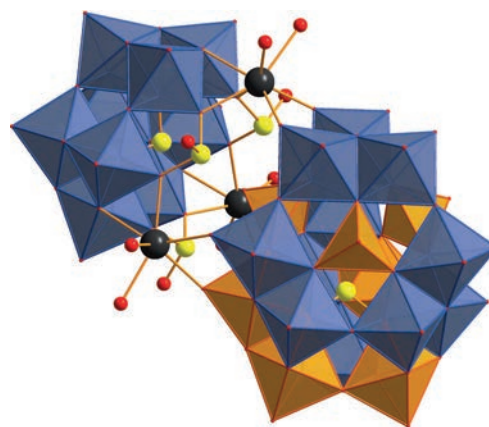


Figure 9. Polyhedral representation of compound **5**. Mo: purple, V: orange, Se: yellow sphere, O: red sphere, and Na: black.

tetrahedra is completed by three  $\mu_3\text{-O}^{2-}$  units and one terminal oxo group  $\text{V}=\text{O}$  with bond lengths between 1.723(8)–1.773(7) Å and 1.611(8)–1.615(8) Å, respectively.

**IR spectroscopy:** Assignment of some diagnostic bands for the mixed-metal (Mo:V) selenite-based polyoxometalates **1–4** are given in Table 3. The bands for the free selenite anion, which exhibits  $C_{3v}$  symmetry, are found in the region of 900–250  $\text{cm}^{-1}$ , where four vibrational modes are observed:  $\nu_1(\text{A}_1)=807$ ,  $\nu_2(\text{A}_1)=432$ ,  $\nu_3(\text{E})=737$  and  $\nu_4(\text{E})=326$   $\text{cm}^{-1}$ .<sup>[31]</sup> However, the symmetry of the selenite anion is lowered to  $C_s$  due to coordination through the oxygen atoms and consequently the doubly degenerate vibration (E) is split into two bands ( $\text{A}' + \text{A}''$ ), which results in the observation of five vibrational modes instead. Additionally, this is not always possible due to the overlap occurring from the vibration bands of the  $\text{M}=\text{O}$  and  $\text{O}-\text{M}-\text{O}$  bonds, which appear in the same region of the IR spectrum. More specifically, the  $\nu(\text{M}=\text{O})$  bands appear in the region 1000–900  $\text{cm}^{-1}$ , leading to an overlap with the  $\text{Se}-\text{O}$  stretching vi-

Table 3. Diagnostic IR bands [ $\text{cm}^{-1}$ ] of compounds **1–4** and of some known metal selenites compounds.

	Coordination modes <sup>[a]</sup> of $\text{SeO}_3^{2-}$	$\nu_1(\text{A}_1)^{[b]}$	$\nu_3(\text{E})$	$\Delta \nu_3-\nu_1 $ [ $\text{cm}^{-1}$ ]	$\nu_2(\text{A}_1)$	$\nu(\text{V}=\text{O})/\nu(\text{Mo}=\text{O})$	Ref.
$\{\text{Mo}_{12}\text{V}_{10}\text{Se}_8\}$ ( <b>1</b> , <b>1'</b> )	$\mu_9\text{-SeO}_3^{2-}$ $(\mu,\mu)\text{-SeO}_3^{2-}$ $(\eta,\mu)\text{-SeO}_3^{2-}$	885 (s)	745 (s)	140	533 (m)	971 (s)/948 (s)	this work
$\{\text{Mo}_{11}\text{V}_7\text{Se}\}$ ( <b>2</b> , <b>2'</b> )	$\mu_9\text{-SeO}_3^{2-}$	898 (m)	747 (m)	151	546 (m)	952 (s)/945 (s)	this work
$\{\text{Mo}_{17}\text{V}_8\text{Se}\}$ ( <b>3</b> )	$\mu_9\text{-SeO}_3^{2-}$	899 (s)	752 (s)	147	589 (s)	972 (s)/955 (s)	this work
$\{\text{Mo}_{20}\text{V}_{16}\text{Se}_{10}\}$ ( <b>4</b> )	$\mu_9\text{-SeO}_3^{2-}$ $(\mu,\mu)\text{-SeO}_3^{2-}$ $(\eta,\eta)\text{-SeO}_3^{2-}$	878 (s)	740 (s)	138	537 (m)	979 (s)/954 (s)	this work
$\text{K}_3[\text{SeS}_3\text{Mo}_6\text{O}_{33}]\cdot 5.5\text{H}_2\text{O}$	$\mu_6\text{-SeO}_3^{2-}$	904 (s)	740 (s)	164	511 (m)	–/930	[32]
$[\text{SeMo}_6\text{O}_{21}(\text{O}_2\text{C}(\text{CH}_2)_2\text{NH}_3)_3]^{2-}$	$\mu_6\text{-SeO}_3^{2-}$	897 (s)	735 (s)	162	507 (m)	–/934	[21]
$[\{\text{Hbipy}\}_3[\text{KM}_9\text{O}_{34}(\text{SeO}_3)_4]]$	$(\eta,\mu,\mu)\text{-SeO}_3^{2-}$	904 (s)	723 (s)	181	539 (m)	–/930	[33]
$[\{\text{H}_2\text{bipy}\}_2[\text{Mo}_9\text{O}_{15}(\text{SeO}_3)_2]]\cdot \text{H}_2\text{O}$	$(\eta,\mu,\mu)\text{-SeO}_3^{2-}$	907 (s)	723 (s)	184	553 (s)	–/932	[33]
$\text{Na}_6[\text{Pd}_{13}\text{Se}_5\text{O}_{32}]\cdot 10\text{H}_2\text{O}$	$\mu_3\text{-SeO}_3^{2-}$	797 (s)	615 (s)	182	549 (m)	–/–	[23a]
$\text{NH}_4[(\text{VO}_2)_3(\text{SeO}_3)_2]$	$\mu_3\text{-SeO}_3^{2-}$	860 (s)	689 (s)	176	560 (w)	941/–	[22b]

[a] See Figures 3 and 8. [b] Intensity codes: s = strong; m = medium; w = weak.

bration bands for compounds **1** and **4**. From Table 3, it is evident that the value of  $|\nu_3 - \nu_1|$ , which expresses the difference between the highest and the lowest Se–O stretching vibration in metal selenite species, is significantly larger for the  $\mu_3$ -SeO<sub>3</sub> coordination mode of the SeO<sub>3</sub><sup>2-</sup> anion<sup>[23a]</sup> (ca. 180 cm<sup>-1</sup> in good agreement with the  $\mu_3$ -(O,O,O) coordination mode of the SO<sub>3</sub><sup>2-</sup> anion<sup>[14b]</sup>) than the  $\mu_6$ -SeO (  $|\nu_3 - \nu_1| \approx 160$  cm<sup>-1</sup>) and  $\mu_9$ -SeO<sub>3</sub> ( $|\nu_3 - \nu_1| \approx 151$  cm<sup>-1</sup> for **2** and 147 cm<sup>-1</sup> for **3**) coordination modes.

Thus, utilisation of FT-IR spectroscopy offers an easy way to distinguish the  $\mu_3$ -SeO<sub>3</sub> from the  $\mu_6$ - and  $\mu_9$ -SeO<sub>3</sub> coordination modes and allows us to make tentative predictions of the material's structural features. Additionally, it can be very useful for identification purposes, by comparing the distinctive regions of the spectra of different selenite-based materials. Even though different types of coordination modes cause different splitting of the vibrational modes, we have to take into consideration that combination of different coordination modes within the same architecture makes it extremely difficult to predict unambiguously the existing coordination modes in a specific material, since only an average splitting between the maximum ( $\mu_3$ -) and the minimum ( $\mu_9$ -) values can ultimately be observed. In the case of compounds **1** and **3**, for example, the peak splitting gives a value of  $|\nu_3 - \nu_1| \approx 140$  and 147 cm<sup>-1</sup>, respectively, and consequently is not possible to determine the type of coordination without having additional information provided by the crystallographic studies. Nevertheless, the technique can still be used effectively in cases in which combinations of coordination modes are present, for identification and comparison purposes.

**ESI-MS spectroscopy:** During the course of this study, ESI-MS,<sup>[34,35]</sup> proved to be a valuable tool in our effort to determine the composition and structural integrity of the {M<sub>22</sub>Se<sub>8</sub>} **1a** and {M<sub>18</sub>Se} **2a** cluster anions in solution unambiguously. This was performed by precipitating the solid by means of ion exchange with tetrabutylammonium (TBA), followed by mass spectroscopic studies in organic solvent (CH<sub>3</sub>CN). The TBA salts of **1a** and **2a** dissolved in CH<sub>3</sub>CN confirmed that the selenite inorganic cages retain their integrity during the course of the MS studies. The main species observed in the case of the {M<sub>22</sub>Se<sub>8</sub>} **1a** cluster anion gave envelopes centered at about *m/z* 2110.9, 2180.0 and 2251.7 and are formulated as [(C<sub>16</sub>H<sub>36</sub>N)<sub>10</sub>K<sub>5</sub>[Mo<sub>12</sub>V<sub>2</sub>V<sup>IV</sup><sub>8</sub>O<sub>58</sub>(SeO<sub>3</sub>)<sub>8</sub>](H<sub>2</sub>O)<sub>6</sub>]<sup>3-</sup>, [(C<sub>16</sub>H<sub>36</sub>N)<sub>11</sub>K<sub>6</sub>[Mo<sub>12</sub>V<sup>IV</sup><sub>10</sub>O<sub>58</sub>(SeO<sub>3</sub>)<sub>8</sub>](H<sub>2</sub>O)<sub>2</sub>]<sup>3-</sup> and [(C<sub>16</sub>H<sub>36</sub>N)<sub>11</sub>K<sub>5</sub>[Mo<sub>12</sub>V<sup>IV</sup><sub>1</sub>V<sup>IV</sup><sub>9</sub>O<sub>58</sub>(SeO<sub>3</sub>)<sub>8</sub>](H<sub>2</sub>O)<sub>16</sub>]<sup>3-</sup>, respectively. For the {M<sub>18</sub>Se} **2a** cluster anion, the higher intensity envelope can be assigned to [(C<sub>16</sub>H<sub>36</sub>N)K<sub>7</sub>H[Mo<sub>11</sub>V<sup>V</sup>V<sup>IV</sup><sub>6</sub>O<sub>52</sub>( $\mu_9$ -SeO<sub>3</sub>)](H<sub>2</sub>O)<sub>20</sub>]<sup>2-</sup> at about *m/z* 1624.7 (Figure 10) and to the dimeric species [(C<sub>16</sub>H<sub>36</sub>N)<sub>5</sub>H<sub>10</sub>[Mo<sub>11</sub>V<sup>V</sup><sub>3</sub>V<sup>IV</sup><sub>4</sub>O<sub>52</sub>( $\mu_9$ -SeO<sub>3</sub>)<sub>2</sub>](H<sub>2</sub>O)<sub>10</sub>]<sup>3-</sup> and [(C<sub>16</sub>H<sub>36</sub>N)<sub>4</sub>K<sub>9</sub>H<sub>8</sub>[Mo<sub>11</sub>V<sup>IV</sup><sub>7</sub>O<sub>52</sub>( $\mu_9$ -SeO<sub>3</sub>)<sub>2</sub>](H<sub>2</sub>O)<sub>17</sub>]<sup>3-</sup> at about *m/z* 2047.6 and 2125.8, respectively. It is worth noting that during the course of the MS studies, we observed a change of the oxidation state of the vanadium centres,<sup>[34b,d]</sup> owing to the high voltages utilised in the mass spectrometry ion-trans-

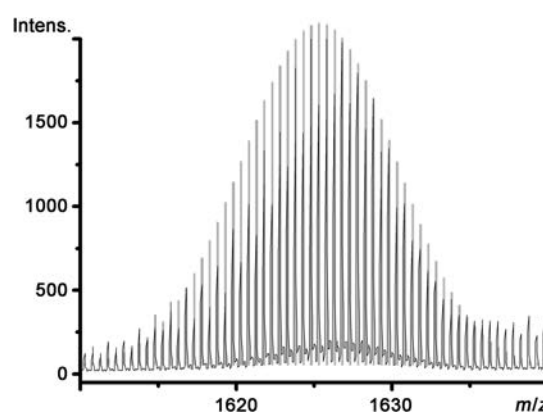


Figure 10. Negative ion mass spectrum of **2a** in acetonitrile. The envelope is centred at *m/z* 1624.7 and can be formulated as [(C<sub>16</sub>H<sub>36</sub>N)K<sub>7</sub>H[Mo<sub>11</sub>V<sup>V</sup>V<sup>IV</sup><sub>6</sub>O<sub>52</sub>( $\mu_9$ -SeO<sub>3</sub>)](H<sub>2</sub>O)<sub>20</sub>]<sup>2-</sup> with six V<sup>IV</sup>. Black line: experimental data, grey line: simulated isotope patterns.

fer process.<sup>[36]</sup> The change of the oxidation state is not unexpected based on previously reported studies on POM systems, in which it has been demonstrated a similar behaviour even for metal centres that are less susceptible to reduction, such as molybdenum and tungsten. Mixed-oxidation-state fragments of polyoxochromate systems have also been identified in solutions during the course of ESI-MS studies.<sup>[37]</sup> In the case of the anions {M<sub>25</sub>Se} **3a** and {M<sub>36</sub>Se<sub>10</sub>} **4a**, the clusters did not retain their integrity in solution during the course of the MS studies and consequently extensive fragmentation has been observed.

## Conclusion

In the present work we reported the discovery, synthesis, structural and spectroscopic characterisation of five unprecedented mixed-metal and mixed-valence selenite-based polyoxometalate anions, namely: {M<sub>22</sub>Se<sub>8</sub>} = [Mo<sup>VI</sup><sub>12</sub>V<sup>V</sup><sub>10</sub>O<sub>58</sub>(SeO<sub>3</sub>)<sub>8</sub>]<sup>10-</sup> (**1a**), {M<sub>18</sub>Se} = [Mo<sup>VI</sup><sub>11</sub>V<sup>V</sup><sub>5</sub>V<sup>IV</sup><sub>2</sub>O<sub>52</sub>( $\mu_9$ -SeO<sub>3</sub>)<sub>7</sub>]<sup>7-</sup> (**2a**), {M<sub>25</sub>Se} = [Mo<sup>VI</sup><sub>11</sub>V<sup>V</sup><sub>5</sub>V<sup>IV</sup><sub>2</sub>O<sub>52</sub>( $\mu_9$ -SeO<sub>3</sub>)(Mo<sub>6</sub>VO<sub>22</sub>)]<sup>10-</sup> (**3a**), {M<sub>36</sub>Se<sub>10</sub>} = [Mo<sup>VI</sup><sub>20</sub>V<sup>V</sup><sub>12</sub>V<sup>IV</sup><sub>4</sub>O<sub>99</sub>(SeO<sub>3</sub>)<sub>10</sub>]<sup>22-</sup> (**4a**) and [Na<sub>3</sub>(H<sub>2</sub>O)<sub>5</sub>{Mo<sub>18-x</sub>V<sub>x</sub>O<sub>52</sub>( $\mu_9$ -SeO<sub>3</sub>)}{Mo<sub>9-y</sub>V<sub>y</sub>O<sub>24</sub>(SeO<sub>3</sub>)<sub>4</sub>}] (**5**). To our knowledge these are the largest Mo/V-selenite-based POMs reported so far. Compounds **1–5** belong to the family of mixed-metal inorganic cages templated by pyramidal (non-conventional) heteroanions. The discovery of novel coordination modes—( $\eta, \mu$ ) and ( $\mu, \mu$ )—of the selenite anion in the structures **1** and **4** demonstrates its ability to act efficiently as inorganic ligand and shows a real potential for the design of novel materials that exhibit unprecedented architectures and potentially interesting properties. The present work completes the series of our initial investigations on the efficiency of pyramidal heteroanions from Group 16 (S, Se, Te) to act as ligands. We have demonstrated that the pyramidal geometry along with the ionic radius of the heteroanions has a profound effect on the self-assembly process of the mixed-metal system and consequently on the structural

features of the isolated product. As the size becomes bigger, an “expansion” of architecture’s volume was observed and higher nuclearity structures were isolated. The average-sized  $\text{SeO}_3^{2-}$  anion proved to be the most diverse, since the fine balance of its ionic radius, charge and geometry gave us the opportunity to isolate a plethora of structures with nuclearities ranging from  $\{\text{M}_{18}\text{Se}\}$  and  $\{\text{M}_{22}\text{Se}_8\}$  to  $\{\text{M}_{25}\text{Se}\}$  and  $\{\text{M}_{36}\text{Se}_{10}\}$ . Furthermore, we demonstrated a design approach by controlling the elegant interplay between the electronic and structural properties of the selenite anion and the effect associated with the counter ions, such as “shrink-wrapping”, hydrogen bonding and solubility of the formed species in solution. The fine control of the above interactions provided access to an extended library of building blocks and finally helped us direct the self-assembly process towards the desired outcome, which gave rise to the isolation of novel archetypes with high nuclearities. ESI-MS studies proved to be decisive for the unambiguous determination of the novel archetypes of the compounds **1** and **2** in solution. Finally, we showed that a detailed FT-IR spectroscopic analysis provides invaluable information regarding the coordination modes of the selenites incorporated in a given compound. The provided data can be very useful in a general case of an unknown material, for which, in combination with the elemental analysis, this could help to identify the existing coordination modes as well as make tentative predictions of its structural features using a simple measurement. In conclusion, the isolation of this family of compounds demonstrates the intriguing interaction that takes place between the metal centres and the selenite anions that promotes the formation of an extremely diverse library of building units and reveals a fascinating potential for further exploration and future discoveries towards the design and synthesis of novel POM-based materials. In the future, we will focus on the investigation of the redox properties of the mixed-metal selenite POMs, identify the effect that the hetero-anion ( $\text{SO}_3^{2-}$ ,  $\text{SeO}_3^{2-}$ ,  $\text{TeO}_3^{2-}$ ) has on the redox behaviour of the material and pave the way towards our efforts to design modular redox active molecular devices.

## Experimental Section

**General:** All chemicals and solvents were purchased from Sigma-Aldrich apart from the  $\text{K}_2\text{SeO}_3$  and  $\text{Na}_2\text{SeO}_3$  salts, which were purchased from Alfa Aesar and were used without further purification. Elemental analyses were completed by using an Elemental Analyser MOD 1106 at University of Glasgow. IR spectra were measured using a JASCO FTIR 410 spectrometer. Thermogravimetric analysis was performed on a TA Instruments Q 500 thermogravimetric analyser under nitrogen or air flow at a typical heating rate of  $5^\circ\text{C min}^{-1}$ . X-ray crystallography diffraction data were collected by means of a Bruker Apex II CCD Diffractometer (150 K). The frame data were acquired with the SMART<sup>[38]</sup> software and  $\text{Mo}_{\text{K}\alpha}$  radiation ( $\lambda = 0.71073 \text{ \AA}$ ). Final values of the cell parameters were obtained from least squares refinement of the positions of all observed reflections. Structure solution and refinement was carried out using SHELXS-97<sup>[39]</sup> and SHELXL-97<sup>[40]</sup> via WinGX.<sup>[41]</sup> Corrections for incident and diffracted beam absorption effects were applied using analytical numeric absorption correction using a multifaceted crystal model.<sup>[42]</sup> Crystallographic parameters for compounds **1–5** are given in Tables 4 and

Table 4. Crystallographic data for compounds **1** and **1'**.

	<b>1</b>	<b>1'</b>
formula	$\text{H}_{36}\text{K}_{10}\text{Mo}_{12}\text{O}_{100}\text{Se}_8\text{V}_{10}$	$\text{H}_{60}\text{K}_4\text{Mo}_{12}\text{N}_6\text{O}_{100}\text{Se}_8\text{V}_{10}$
$M_r$ [ $\text{g mol}^{-1}$ ]	4319.65	4193.30
symmetry	monoclinic	monoclinic
space group	$C2/m$	$C2/c$
$a$ [ $\text{\AA}$ ]	37.717(2)	28.1611(9)
$b$ [ $\text{\AA}$ ]	13.3912(7)	10.9062(3)
$c$ [ $\text{\AA}$ ]	10.5375(6)	32.9468(12)
$\alpha$ [ $^\circ$ ]	90	90
$\beta$ [ $^\circ$ ]	104.169(6)	105.586(4)
$\gamma$ [ $^\circ$ ]	90	90
$\rho_{\text{calcd}}$ [ $\text{g cm}^{-3}$ ]	2.780	2.858
$V$ [ $\text{\AA}^3$ ]	5160.4(5)	9746.9(5)
$Z$	2	4
$\mu$ [ $\text{mm}^{-1}$ ]	26.689	5.683
$T$ [K]	150(2)	150(2)
rfIns (measured)	9505	39936
rfIns (unique)	2978	8012
$R_1$	0.0756	0.0593
$wR_2$ (all data)	0.1969	0.1638
GooF, $S$	1.076	0.936

5. Further details of the crystal structure investigations of compounds **1–5** can be obtained from FIZ Karlsruhe, 76344 Eggenstein-Leopoldshafen, Germany, (fax: (+49) 7247–808–666; e-mail: crysdata@fiz.karlsruhe.de) on quoting the depository numbers CSD-424242 (**1**), CSD-424243 (**1'**), CSD-424244 (**2'**), CSD-424245 (**2**), CSD-424246 (**3**), CSD-424247 (**4**), and CSD-424248 (**5**). ESI-MS measurements were carried out at  $180^\circ\text{C}$ . The solutions of the samples were diluted so that the maximum concentration of the cluster ions was of the order of  $10^{-5}\text{M}$  and these were infused at a flow rate of  $180 \mu\text{L h}^{-1}$ . The mass spectrometer used for the measurements was a Bruker micro TOF-Q and the data were collected in negative mode. The spectrometer was previously calibrated with the standard tune mix to give a precision of about 1.5 ppm in the region of 500–5000  $m/z$ . The standard parameters for a medium mass data acquisition were used. Typical working conditions: the end plate voltage was set to  $-500 \text{ V}$  and the capillary to  $-3500 \text{ V}$ ; the collision cell was set to collision energy  $-10.0 \text{ eV z}^{-1}$  with a maximum gas flowrate of  $4.0 \text{ L h}^{-1}$ .

**Synthesis of  $\text{K}_{10}[\text{Mo}^{\text{VI}}_{12}\text{V}^{\text{V}}_{10}\text{O}_{88}(\text{SeO}_3)_8]\cdot 18\text{H}_2\text{O}$  (**1**):**  $\text{K}_2\text{MoO}_4$  (0.67 g, 2.8 mmol) was dissolved in deionised water (25 mL). Then solid  $\text{KVO}_3$  (0.70 g, 5.1 mmol) was added in one portion to the solution under stirring and the resulting solution was heated to  $90^\circ\text{C}$  for 10 min, during which time the vanadate salt completely dissolved. Solid  $\text{K}_2\text{SeO}_3$  (0.19 g, 0.93 mmol) and  $\text{NH}_2\text{NH}_2\cdot 2\text{HCl}$  (0.0042 g, 0.04 mmol) were successively added under stirring and the pH was adjusted by drop-wise addition of 3M HCl after the reaction was cooled down at room temperature. Compound **1** was isolated between pH 0.5 and 2.5. The optimum yield obtained at pH value of 1.5. The dark brown solution was filtered off and the filtrate left in an open vessel (a 100 mL beaker) at room temperature (ca.  $20^\circ\text{C}$ ) for two days, during which time dark orange crystals suitable for X-ray structure analysis were obtained. Yield: 0.271 g (27% based on Mo); IR (KBr):  $\tilde{\nu} = 3425$  (br), 1623 (s), 964 (s), 879 (s), 803 (s), 746 (s), 699 (s),  $564 \text{ cm}^{-1}$  (s); elemental analysis calcd (%) for  $\text{H}_{36}\text{K}_{10}\text{Mo}_{12}\text{O}_{100}\text{Se}_8\text{V}_{10}$  (4319.5): Mo 26.65, V 11.79, Se 14.62, K 9.05; found: Mo 26.75, V 11.44, Se 14.33, K 9.14.

**Synthesis of  $(\text{NH}_4)_6\text{K}_4[\text{Mo}^{\text{VI}}_{12}\text{V}^{\text{V}}_{10}\text{O}_{88}(\text{SeO}_3)_8]\cdot 18\text{H}_2\text{O}$  (**1'**):** Solid  $\text{NH}_4\text{VO}_3$  (0.40 g, 3.4 mmol) was added in one portion to a stirred solution of  $(\text{NH}_4)_6\text{Mo}_7\text{O}_{24}\cdot 4\text{H}_2\text{O}$  (0.60 g, 0.4 mmol) in water (25 mL), and the resulting solution was heated to  $90^\circ\text{C}$  until the vanadate salt completely dissolved. The reaction is allowed to cool down at room temperature and then solid  $\text{K}_2\text{SeO}_3$  (0.19 g, 0.93 mmol) was added. After 5 min of stirring  $\text{NH}_2\text{NH}_2\cdot 2\text{HCl}$  (0.0042 g, 0.04 mmol) was slowly added. The reaction mixture was stirred for 10 min and the pH was adjusted to 1.5 by addition of concentrated HCl to the solution. The dark brown solution was filtered and the filtrate was left to crystallise for two weeks in an open

Table 5. Crystallographic data for compounds 2–5.

	2	2'	3	4	5
formula	H <sub>74</sub> K <sub>3</sub> Mo <sub>11</sub> N <sub>4</sub> O <sub>84</sub> SeV <sub>7</sub>	H <sub>62</sub> K <sub>7</sub> Mo <sub>11</sub> O <sub>86</sub> SeV <sub>7</sub>	H <sub>108</sub> K <sub>3</sub> Mo <sub>17</sub> N <sub>7</sub> O <sub>117</sub> SeV <sub>8</sub>	H <sub>148</sub> K <sub>3</sub> Mo <sub>20</sub> N <sub>19</sub> O <sub>165</sub> Se <sub>10</sub> V <sub>16</sub>	H <sub>90</sub> Mo <sub>16</sub> N <sub>13</sub> Na <sub>3</sub> O <sub>106</sub> Se <sub>5</sub> V <sub>11</sub>
<i>M<sub>r</sub></i> [g mol <sup>-1</sup> ]	3082.81	3203.08	4313.69	6696.11	4556.02
symmetry	rhombohedral	tetragonal	orthorhombic	monoclinic	triclinic
space group	<i>R</i> 3̄c	<i>P</i> 4̄b2	<i>Pnma</i>	<i>P</i> 2 <sub>1</sub> / <i>m</i>	<i>P</i> 1̄
<i>a</i> [Å]	14.1424(2)	25.7061(2)	15.4044(6)	16.0462(2)	14.2068(2)
<i>b</i> [Å]	14.1424(2)	25.7061(2)	21.3761(9)	27.9052(4)	20.4415(4)
<i>c</i> [Å]	127.7889(4)	19.9182(2)	25.8412(10)	20.9112(2)	22.2928(3)
<i>α</i> [°]	90	90	90	90	93.1140(10)
<i>β</i> [°]	90	90	90	94.1060(10)	93.3370(10)
<i>γ</i> [°]	120	90	90	90	105.596(2)
<i>ρ</i> <sub>calcd</sub> [g cm <sup>-3</sup> ]	2.775	3.233	3.367	2.381	2.437
<i>V</i> [Å <sup>3</sup> ]	22134.5(4)	13162.0(2)	8509.1(6)	9339.4(2)	6208.57(17)
<i>Z</i>	12	8	4	2	2
<i>μ</i> [mm <sup>-1</sup> ]	3.443	30.548	30.168	20.874	3.927
<i>T</i> [K]	150(2)	150(2)	150(2)	150(2)	150(2)
rflns (measured)	74173	50907	26149	70886	100614
rflns (unique)	3839	11667	6904	16230	24407
<i>R</i> 1	0.0513	0.0685	0.0698	0.0619	0.0666
w <i>R</i> 2 (all data)	0.1718	0.1882	0.2041	0.1652	0.1988
Goof, <i>S</i>	1.028	1.115	1.067	1.025	1.068

vessel at room temperature. Dark orange crystals were filtered and dried in air. Yield: 0.253 g (26% based on Mo); IR (KBr):  $\tilde{\nu}$  = 3444 (br), 1611 (s), 1402 (s), 971 (s), 863 (s), 754 (s), 665 (s), 569 (s), 533 cm<sup>-1</sup> (s); elemental analysis calcd (%) for H<sub>60</sub>K<sub>4</sub>Mo<sub>12</sub>N<sub>6</sub>O<sub>100</sub>Se<sub>8</sub>V<sub>10</sub> (4193.12): Mo 27.46, V 12.15, Se 15.06, K 3.76, N: 2.00; found: Mo 27.10, V 12.31, Se 15.00, K 3.77, N 2.23.

**Synthesis of (NH<sub>4</sub>)<sub>3</sub>K<sub>3</sub>[Mo<sup>VI</sup><sub>11</sub>V<sup>V</sup><sub>5</sub>V<sup>IV</sup><sub>2</sub>O<sub>52</sub>(SeO<sub>3</sub>)]·29H<sub>2</sub>O (2')** The same procedure as for the above compound 1' was followed to prepare 2', but the pH was adjusted to 4.0 by addition of concentrated HCl to the solution. The dark green solution was filtered and the filtrate was left to crystallise for two weeks in an open vessel at room temperature. The green hexagonal crystals were filtered and dried in air. Yield: 0.314 g (41% based on Mo); IR (KBr):  $\tilde{\nu}$  = 3444 (br), 1401 (s), 952 (s), 862 (s), 818 (s), 747 (s), 580 (s), 546 cm<sup>-1</sup> (s); elemental analysis calcd (%) for H<sub>74</sub>K<sub>3</sub>Mo<sub>11</sub>N<sub>4</sub>O<sub>84</sub>Se<sub>7</sub>V<sub>7</sub> (3082.6): Mo 34.23, V 11.57, Se 2.58, K 3.80, N: 1.82; found: Mo 34.41, V 11.80, Se 2.88, K 3.69, N 1.97.

**Synthesis of K<sub>7</sub>[Mo<sup>VI</sup><sub>11</sub>V<sup>V</sup><sub>5</sub>V<sup>IV</sup><sub>2</sub>O<sub>52</sub>(SeO<sub>3</sub>)]·31H<sub>2</sub>O (2)** The same procedure as for the above compound 1 was followed to prepare 2 but the pH was adjusted by drop-wise addition of 3 M HCl to 3. The dark brown solution was filtered off and the filtrate left in an open vessel (a 100 mL beaker) at room temperature (ca. 25 °C) for one week, during which time brown hexagonal crystals suitable for X-ray structure analysis were obtained. Yield: 0.155 g (20% based on Mo); IR (KBr):  $\tilde{\nu}$  = 3454 (br), 1618 (s), 964 (s), 858 (s), 814 (s), 747 (s), 568 cm<sup>-1</sup> (s); elemental analysis calcd (%) for H<sub>62</sub>K<sub>7</sub>Mo<sub>11</sub>O<sub>86</sub>SeV<sub>7</sub> (3202.92): Mo 32.98, V 11.13, Se 2.47, K 8.54; found: Mo 33.41, V 11.21, Se 2.36, K 8.71.

**Synthesis of (NH<sub>4</sub>)<sub>7</sub>K<sub>3</sub>[Mo<sup>VI</sup><sub>11</sub>V<sup>V</sup><sub>5</sub>V<sup>IV</sup><sub>2</sub>O<sub>52</sub>(SeO<sub>3</sub>)(Mo<sub>6</sub>VO<sub>22</sub>)]·40H<sub>2</sub>O (3)** The same procedure as for the above compound 1' was followed to prepare 3, but the pH was adjusted to 2.8 by addition of concentrated HCl to the solution. The dark green solution was filtered and the filtrate was left to crystallise for two weeks in an open vessel at room temperature, during which time dark green needles along with big hexagonal crystals of compound 3 suitable for X-ray structure analysis were obtained. The needle-shaped crystals were separated manually under a microscope. The separation of the crystals is relatively easy due to considerably different size and shape of the two sets of crystals. Yield: 0.131 g (ca. 19% based on Mo); IR (KBr):  $\tilde{\nu}$  = 3433 (br), 1402 (s), 966 (s), 905 (s), 862 (s), 762 (s), 589 (s), 480 (s), 461 cm<sup>-1</sup> (s); elemental analysis calcd (%) for H<sub>108</sub>K<sub>3</sub>Mo<sub>17</sub>N<sub>7</sub>O<sub>117</sub>Se<sub>1</sub>V<sub>8</sub> (4313.45): Mo 37.81, V 9.45, Se 1.83, K 2.72, N: 2.27; found: Mo: 37.52, V: 9.53, Se: 2.01, K: 2.95, N: 2.39.

**Synthesis of (NH<sub>4</sub>)<sub>19</sub>K<sub>3</sub>[Mo<sup>VI</sup><sub>20</sub>V<sup>V</sup><sub>12</sub>V<sup>IV</sup><sub>4</sub>O<sub>99</sub>(SeO<sub>3</sub>)<sub>10</sub>]·36H<sub>2</sub>O (4)** The same procedure as for the above compound 1' was followed to prepare 4, but the pH was adjusted to 5.0 by addition of concentrated HCl to the solu-

tion. The dark green solution was filtered and the filtrate was left to stand for two weeks in an open vessel at room temperature, during which time green hexagonal-shaped crystals suitable for X-ray structure analysis were obtained. Yield: 0.10 g (ca. 11% based on Mo); IR (KBr):  $\tilde{\nu}$  = 3434 (br), 1615 (s), 1399 (s), 954 (s), 852 (s), 727 (s), 579 (s), 537 cm<sup>-1</sup> (s); elemental analysis calcd (%) for H<sub>148</sub>K<sub>3</sub>Mo<sub>20</sub>N<sub>19</sub>O<sub>165</sub>Se<sub>10</sub>V<sub>16</sub> (6695.78): Mo 28.65, V 12.17, Se 11.79, K 1.75, N: 3.97; found: Mo: 28.89, V: 11.65, Se: 11.91, K: 1.68, N 4.10. The higher content of N can be assigned to the excess of NH<sub>4</sub>Cl that co-crystallises with compound 4.

**Synthesis of [Na<sub>3</sub>(H<sub>2</sub>O)<sub>3</sub>{Mo<sub>11</sub>V<sub>7</sub>O<sub>52</sub>(μ<sub>9</sub>-SeO<sub>3</sub>)}{Mo<sub>5</sub>V<sub>4</sub>O<sub>24</sub>(SeO<sub>3</sub>)<sub>4</sub>}] (5)** Solid NH<sub>4</sub>VO<sub>3</sub> (0.40 g, 3.4 mmol) was added in one portion to a stirred solution of (NH<sub>4</sub>)<sub>6</sub>Mo<sub>7</sub>O<sub>24</sub>·4H<sub>2</sub>O (0.60 g, 0.4 mmol) in water (25 mL) and the resulting solution was heated to 90 °C until the vanadate salt completely dissolved. The reaction is allowed to cool down at room temperature and then solid Na<sub>2</sub>SeO<sub>3</sub> (0.21 g, 0.93 mmol) was added. After 5 min of stirring NH<sub>2</sub>NH<sub>2</sub>·2HCl (0.0042 g, 0.04 mmol) was slowly added. The reaction mixture was stirred for 10 min and the pH was adjusted between 2.5 and 4 by addition of concentrated HCl to the solution. The dark green solution was filtered and the filtrate was left to crystallise for two weeks in an open vessel at room temperature.

## Acknowledgements

This work was supported by the EPSRC, WestCHEM and The University of Glasgow. H.N.M thanks the Royal Society of Edinburgh and Marie Curie Actions for financial support. L.C. thanks the Royal Society and Wolfson Foundation for a merit award.

- [1] a) M. T. Pope, A. Muller, *Angew. Chem.* **1991**, *103*, 56–70; *Angew. Chem. Int. Ed. Engl.* **1991**, *30*, 34–48; b) special issue on polyoxometalates, *Chem. Rev.* **1998**, *98*, 1–387; c) B. Hasenknopf, *Front. Biosci.* **2005**, *10*, 275–287; d) D.-L. Long, E. Burkholder, L. Cronin, *Chem. Soc. Rev.* **2007**, *36*, 105–121; e) D.-L. Long, R. Tsunashima, L. Cronin, *Angew. Chem.* **2010**, *122*, 1780–1803; *Angew. Chem. Int. Ed.* **2010**, *49*, 1736–1758.
- [2] a) *Heteropoly and Isopoly Oxometalates* (Ed.: M. T. Pope), Springer, New York (USA), **1983**; b) *Metal Oxide Chemistry and Synthesis: From Solution to Solid State* (Ed.: J. P. Jolivet), Wiley, New York (USA), **2000**; c) *Polyoxometalate Chemistry for Nanocomposite Design* (Eds.: M. T. Pope, T. Yamase), Kluwer, Dordrecht (The

- Netherlands), **2002**; d) *Polyoxometalates: From Topology via Self-Assembly to Applications* (Eds.: M. T. Pope, A. Müller), Kluwer, Dordrecht (The Netherlands), **2001**.
- [3] G. Chaidogiannos, D. Velessiotis, P. Argitis, P. Koutsoloulos, C. D. Diakoumakos, D. Tsamakidis, N. Glezos, *Microelectron. Eng.* **2004**, *73–74*, 746–751.
- [4] M. Luban, F. Borsa, S. Bud'ko, P. Canfield, S. Jun, J. K. Jung, P. Kögerler, D. Mentrup, A. Müller, R. Modler, D. Prociassi, B. J. Suh, M. Torikachvili, *Phys. Rev. B* **2002**, *66*, 054407.
- [5] a) M. Ibrahim, Y. Lan, B. S. Bassil, Y. Xiang, A. Suchopar, A. K. Powell, U. Kortz, *Angew. Chem.* **2011**, *123*, 4805–4808; *Angew. Chem. Int. Ed.* **2011**, *50*, 4708–4711; b) C. Ritchie, A. Ferguson, H. Nojiri, H. N. Miras, Y. F. Song, D.-L. Long, E. Burkholder, M. Murrie, P. Kögerler, E. K. Brechin, L. Cronin, *Angew. Chem.* **2008**, *120*, 5691–5694; *Angew. Chem. Int. Ed.* **2008**, *47*, 5609–5612; c) J.-D. Compain, P. Mialane, A. Dolbecq, I. M. Mbomekalle, J. Marrot, F. Sécheresse, E. Rivière, G. Rogez, W. Wernsdorfer, *Angew. Chem.* **2009**, *121*, 3123–3127; *Angew. Chem. Int. Ed.* **2009**, *48*, 3077–3081.
- [6] a) I. M. Mbomekalle, B. Keita, L. Nadjo, P. Berthet, K. I. Hardcastle, C. L. Hill, T. M. Anderson, *Inorg. Chem.* **2003**, *42*, 1163–1169; b) M. V. Vasylyev, R. Neumann, *J. Am. Chem. Soc.* **2004**, *126*, 884–890; c) R. Neumann, A. M. Khenkin, I. Vigdergauz, *Chem. Eur. J.* **2000**, *6*, 875–882; d) N. Mizuno, K. Yamaguchi, K. Kamata, *Coord. Chem. Rev.* **2005**, *249*, 1944–1956.
- [7] a) K. Nomiya, H. Torii, T. Hasegawa, Y. Nemoto, K. Nomura, K. Hashino, M. Uchida, Y. Kato, K. Shimizu, M. Oda, *J. Inorg. Biochem.* **2001**, *86*, 657–667; b) J. T. Rhule, C. L. Hill, D. A. Judd, *Chem. Rev.* **1998**, *98*, 327–358.
- [8] D.-L. Long, H. Abbas, P. Kögerler, L. Cronin, *J. Am. Chem. Soc.* **2004**, *126*, 13880–13881.
- [9] H. N. Miras, G. J. T. Cooper, D.-L. Long, H. Bögger, A. Müller, C. Streb, L. Cronin, *Science* **2010**, *327*, 72–74.
- [10] a) S. G. Mitchell, C. Ritchie, D.-L. Long, L. Cronin, *Dalton Trans.* **2008**, 1415–1417; b) J. Thiel, C. Ritchie, H. N. Miras, C. Streb, S. G. Mitchell, T. Boyd, M. N. C. Ochoa, M. H. Rosnes, J. McIver, D.-L. Long, L. Cronin, *Angew. Chem.* **2010**, *122*, 7138–7142; *Angew. Chem. Int. Ed.* **2010**, *49*, 6984–6988; c) J. Thiel, C. Ritchie, C. Streb, D.-L. Long, L. Cronin, *J. Am. Chem. Soc.* **2009**, *131*, 4180–4181; d) J. Yan, D. L. Long, H. N. Miras, L. Cronin, *Inorg. Chem.* **2010**, *49*, 1819–1825.
- [11] a) T. M. Anderson, X. Zhang, K. I. Hardcastle, C. L. Hill, *Inorg. Chem.* **2002**, *41*, 2477–2488; b) Y. V. Geletii, C. L. Hill, A. J. Bailey, K. I. Hardcastle, R. H. Atalla, I. A. Weinstock, *Inorg. Chem.* **2005**, *44*, 8955–8966; c) J. Zhang, D. Li, G. Liu, K. J. Glover, T. Liu, *J. Am. Chem. Soc.* **2009**, *131*, 15152–15159; d) S. J. Veen, W. K. Kegel, *J. Phys. Chem. B* **2009**, *113*, 15137–15140.
- [12] a) K. Y. Matsumoto, M. Kato, Y. Sasaki, *Bull. Chem. Soc. Jpn.* **1976**, *49*, 106–110; b) T. Kudo, *Nature* **1984**, *312*, 537–538; c) C. Robl, K. Haake, *J. Chem. Soc. Chem. Commun.* **1993**, 397–399; d) *Molecular Engineering, Vol. 3* (Eds.: B. Krebs, R. Klein) SpringerLink, Heidelberg (Germany), **1993**, pp. 43–59; e) L. Cronin, in *Comprehensive Coordination Chemistry II* (Eds.: J. A. McCleverty, T. J. Meyer) **2004**, pp. 1–57; f) N. Belai, M. T. Pope, *Chem. Commun.* **2005**, 5760–5762.
- [13] a) D.-L. Long, H. Abbas, P. Kögerler, L. Cronin, *Angew. Chem.* **2005**, *117*, 3481–3485; *Angew. Chem. Int. Ed.* **2005**, *44*, 3415–3419; b) C. Baffert, S. W. Feldberg, A. M. Bond, D. L. Long, L. Cronin, *Dalton Trans.* **2007**, 4599–4607; c) N. Fay, A. Bond, C. Baffert, J. Boas, J. Pilbrow, D.-L. Long, L. Cronin, *Inorg. Chem.* **2007**, *46*, 3502–3510.
- [14] a) M. J. Manos, H. N. Miras, V. Tangoulis, J. D. Woolins, A. M. Z. Slawin, T. A. Kabanos, *Angew. Chem.* **2003**, *115*, 441–443; *Angew. Chem. Int. Ed.* **2003**, *42*, 425–427; b) H. N. Miras, R. G. Raptis, P. Baran, N. Lalioti, M. P. Sigalas, T. A. Kabanos, *Chem. Eur. J.* **2005**, *11*, 2295–2306; c) H. N. Miras, R. Raptis, P. Baran, N. Lalioti, A. Harrison, T. A. Kabanos, *C. R. Chim.* **2005**, *8*, 957–962; d) H. N. Miras, D. J. Stone, E. J. L. McInnes, R. G. Raptis, P. Baran, G. I. Chilias, M. P. Sigalas, T. A. Kabanos, L. Cronin, *Chem. Commun.* **2008**, 4703–4705; e) H. N. Miras, M. N. C. Ochoa, D.-L. Long, L. Cronin, *Chem. Commun.* **2010**, 46, 8148–8150; f) M. N. Corella-Ochoa, H. N. Miras, A. Kidd, D.-L. Long, L. Cronin, *Chem. Commun.* **2011**, *47*, 8799–8801; g) R. Canioni, C. Marchal-Roch, N. Leclerc-Laronze, M. Haouas, F. Taulèlle, J. Marrot, S. Paul, C. Lamonier, J.-F. Paul, S. Loridant, J.-M. M. Millet, E. Cadot, *Chem. Commun.* **2011**, *47*, 6413–6415.
- [15] a) K. Nomiya, T. Takahashi, T. Shirai, M. Miwa, *Polyhedron* **1987**, *6*, 213–218; b) C. P. A. Lorenzo-Luis, P. Gili, A. Sánchez, E. Rodriguez-Castellón, J. Jiménez-Jiménez, C. Ruiz-Pérez, X. Solans, *Transition Met. Chem.* **1999**, *24*, 686–692; c) Y. Li, E. Wang, S. Wang, Y. Duan, C. Hu, N. Hu, H. Jia, *J. Mol. Struct.* **2002**, *611*, 185–191; d) D. Honda, S. Ikegami, T. Inoue, T. Ozeki, A. Yagasaki, *Inorg. Chem.* **2007**, *46*, 1464–1470; e) F.-X. Liu, C. Marchal-Roch, D. Dambournet, A. Acker, J. Marrot, F. Sécheresse, *Eur. J. Inorg. Chem.* **2008**, 2191–2198.
- [16] a) J. F. Keggin, *Proc. R. Soc. London Ser. A* **1934**, *144*, 75–100; b) X. López, C. Bo, J. M. Poblet, *J. Am. Chem. Soc.* **2002**, *124*, 12574–12582; c) C. M. Liu, D.-Q. Zhang, D.-B. Zhu, *Cryst. Growth Dec.* **2006**, *6*, 524–529; d) C. Streb, C. Ritchie, D.-L. Long, P. Kögerler, L. Cronin, *Angew. Chem.* **2007**, *119*, 7723–7726; *Angew. Chem. Int. Ed.* **2007**, *46*, 7579–7582; e) S. G. Mitchell, S. Khanra, H. N. Miras, T. Boyd, D.-L. Long, L. Cronin, *Chem. Commun.* **2009**, 2712–2714.
- [17] a) E.-B. Wang, B.-T. Li, Z.-P. Wang, B.-J. Zhang, *Chem. Res. Chin. Univ.* **1996**, *12*, 322–325; b) L. E. Briand, G. T. Baronetti, H. J. Thomas, *Appl. Catal. A* **2003**, *256*, 37–50; c) N. Leclerc-Laronze, J. Marrot, G. Herve, *Inorg. Chem.* **2005**, *44*, 1275–1281; d) T. Boyd, S. G. Mitchell, H. N. Miras, D.-L. Long, L. Cronin, *Dalton Trans.* **2010**, 39, 6460–6465.
- [18] D.-L. Long, Y.-F. Song, E. F. Wilson, P. Kögerler, S.-X. Guo, A. M. Bond, J. S. J. Hargreaves, L. Cronin, *Angew. Chem.* **2008**, *120*, 4456–4459; *Angew. Chem. Int. Ed.* **2008**, *47*, 4384–4387.
- [19] D.-L. Long, P. Kögerler, L. Cronin, *Angew. Chem.* **2004**, *116*, 1853–1856; *Angew. Chem. Int. Ed.* **2004**, *43*, 1817–1820.
- [20] a) Y. Ozawa, Y. Sasaki, *Chem. Lett.* **1987**, *16*, 923–926; b) Y. Jeanin, J. Martin-Frère, *Inorg. Chem.* **1979**, *18*, 3010–3014; c) J. Yan, D.-L. Long, L. Cronin, *Angew. Chem.* **2010**, *122*, 4211–4214; *Angew. Chem. Int. Ed.* **2010**, *49*, 4117–4120; d) J. Yan, J. Gao, D.-L. Long, H. N. Miras, L. Cronin, *J. Am. Chem. Soc.* **2010**, *132*, 11410–11411.
- [21] U. Kortz, M. G. Savelieff, F. Y. A. Ghali, L. M. Khalil, S. A. Maalouf, D. I. Sinno, *Angew. Chem.* **2002**, *114*, 4246–4249; *Angew. Chem. Int. Ed.* **2002**, *41*, 4070–4073.
- [22] a) S.-Y. Zhang, C.-L. Hu, C.-F. Sun, J.-G. Mao, *Inorg. Chem.* **2010**, *49*, 11627–11636; b) J. T. Vaughey, W. T. A. Harrison, L. L. Dussack, A. J. Jacobson, *Inorg. Chem.* **1994**, *33*, 4370–4375.
- [23] a) N. V. Izarova, M. H. Dickman, R. N. Biboum, B. Keita, L. Nadjo, V. Ramachandran, N. S. Dalal, U. Lortz, *Inorg. Chem.* **2009**, *48*, 7504–7506; b) M. Delferro, C. Graiff, L. Elviri, G. Predieri, *Dalton Trans.* **2010**, 39, 4479–4481; c) N. V. Izarova, A. Banerjee, U. Kortz, *Inorg. Chem.* **2011**, *50*, 10379–10386.
- [24] N. I. Kapakoglou, P. I. Betzios, S. E. Kazianis, C. E. Kosmidis, C. Drouza, M. J. Manos, M. P. Sigalas, A. D. Keramidis, T. A. Kabanos, *Inorg. Chem.* **2007**, *46*, 6002–6010.
- [25] a) D.-L. Long, P. Kögerler, L. J. Farrugia, L. Cronin, *Angew. Chem.* **2003**, *115*, 4312–4315; *Angew. Chem. Int. Ed.* **2003**, *42*, 4180–4183; b) C. P. Pradeep, D.-L. Long, L. Cronin, *Dalton Trans.* **2010**, 39, 9443–9457.
- [26] A. Björnberg, *Acta Crystallogr. Sect. B* **1980**, *36*, 1530–1536.
- [27] a) H. T. Evans, *Inorg. Chem.* **1966**, *5*, 967–977; b) E. Coronado, J. R. Galan-Mascaros, C. Gimenez-Saiz, C. J. Gomez-Garcia, E. Martinez-Ferrero, M. Almeida, E. B. Lopes, *Adv. Mater.* **2004**, *16*, 324–327; c) A. Dewan, D. K. Kakati, B. K. Das, *Indian J. Chem. A* **2010**, *49*, 39–44.
- [28] H. N. Miras, J. Yan, D.-L. Long, L. Cronin, *Angew. Chem.* **2008**, *120*, 8548–8551; *Angew. Chem. Int. Ed.* **2008**, *47*, 8420–8423.
- [29] a) R. D. Shannon, *Acta Crystallogr. Sect. A* **1976**, *32*, 751–767; b) I. D. Brown, in *Structure and Bonding in Crystals, Vol II* (Eds.: M. O'Keefe, A. Navrotsky), Academic Press, New York (USA), **1981**, pp. 1–30; c) I. D. Brown, *Chem. Rev.* **2009**, *109*, 6858–6919.

- [30] a) A. Müller, E. Krickemeyer, S. Dillinger, J. Meyer, H. Bögge, A. Stammler, *Angew. Chem.* **1996**, *108*, 183–185; *Angew. Chem. Int. Ed. Engl.* **1996**, *35*, 171–173; b) M. Bösing, I. Loose, H. Pohlmann, B. Krebs, *Chem. Eur. J.* **1997**, *3*, 1232–1237.
- [31] P. K. Nakamoto, *Infrared and Raman Spectra of Inorganic and Coordination Compounds*, Wiley, New York (USA), **2009**.
- [32] C. Robl, K. Haake, *J. Chem. Soc. Chem. Commun.* **1993**, 397–399.
- [33] M.-L. Feng, J.-G. Mao, *Eur. J. Inorg. Chem.* **2004**, 3712–3717.
- [34] a) H. N. Miras, E. F. Wilson, L. Cronin, *Chem. Commun.* **2009**, 1297–1311; b) H. N. Miras, D.-L. Long, P. Kögerler, L. Cronin, *Dalton Trans.* **2008**, 214–221; c) E. F. Wilson, H. N. Miras, M. H. Rosnes, L. Cronin, *Angew. Chem.* **2011**, *123*, 3804–3808; *Angew. Chem. Int. Ed.* **2011**, *50*, 3720–3724; d) H. N. Miras, Daniel Stone, D.-L. Long, E. J. L. McInnes, P. Kögerler, L. Cronin, *Inorg. Chem.* **2011**, *50*, 8384–8391; e) H. N. Miras, H. Y. Zang, D.-L. Long, L. Cronin, *Eur. J. Inorg. Chem.* **2011**, 5105–5111.
- [35] a) M. Bonchio, O. Bortolini, V. Conte, A. Sartorel, *Eur. J. Inorg. Chem.* **2003**, 699–704; b) D. K. Walanda, R. C. Burns, G. A. Lawrance, E. I. von Nagy-Felsobuki, *J. Chem. Soc. Dalton Trans.* **1999**, 311–321; c) J. Gun, A. Modestov, O. Lev, D. Saurenx, M. A. Vorotyntsev, R. Poli, *Eur. J. Inorg. Chem.* **2003**, 482–492; d) M. J. Deery, O. W. Howarth, K. R. J. Jennings, *Chem. Soc. Dalton Trans.* **1997**, 4783–4788; e) S. Sakamoto, M. Fujita, K. Kim, K. Yamaguchi, *Tetrahedron* **2000**, *56*, 955–964.
- [36] E. F. Wilson, H. Abbas, B. J. Duncombe, C. Streb, D.-L. Long, L. Cronin, *J. Am. Chem. Soc.* **2008**, *130*, 13876–13884.
- [37] F. Sahureka, R. C. Burns, E. I. von Nagy-Felsobuki, *Inorg. Chim. Acta* **2002**, *332*, 7–17.
- [38] SMART-NT Software Reference Manual, version 5.059, Bruker AXS, Inc., Madison, WI, **1998**.
- [39] G. M. Sheldrick, *Acta Crystallogr. Sect. A* **1990**, *46*, 467–473.
- [40] G. M. Sheldrick, *Acta Crystallogr. Sect. A* **2008**, *64*, 112–122.
- [41] L. J. J. Farrugia, *Appl. Crystallogr.* **1999**, *32*, 837–838.
- [42] R. C. Clark, J. S. Reid, *Acta Crystallogr. Sect. A* **1995**, *51*, 887–897.

Received: March 19, 2012  
Published online: September 20, 2012